Supplementary Material

Text S1. Variability in GMSL contributions for different ice margins versus Earth models
In Figure 4, we compare GMSL contributions and ice volumes from our ICE-NADI-1 ice sheet thickness reconstructions alongside the ICE-7G (Roy & Peltier, 2017), NAICE (Gowan et al., 2016b), and LW-6 (Lambeck et al., 2017) reconstructions. The greatest differences in ice sheet geometry among our new reconstructions arises when different NADI-1 margins are adopted rather than different viscoelastic Earth models. For instance, in reconstructions adopting the NADI-1 optimal margins, we find average differences of 0.3-1.0 m GMSL from 25 ka to present among simulations adopting different Earth models. In contrast, simulations that use the same Earth model (either Earth_1 or Earth_2) but adopt the NADI-1 optimal, minimum, or maximum margins yield average differences of 5.1 – 12.8 m in GMSL (Fig. 4).

Text S2. Relative Sea Level
Among the regions with sea-level compilations considered in this study, the largest differences in RSL predictions from the three ICE-NADI-1 reconstructions occur along the eastern Canadian coastline. From 16 ka to present, the time interval over which RSL observations are primarily available along the eastern Canadian coastline, average RSL predictions differ by 22 m between the ICE-NADI-1 reconstruction and both the ICE-NADI-1_min and ICE-NADI-1_max reconstructions (Figs. 6-7, S4-S9). A key source of these discrepancies is the large uncertainty bounds in the NADI-1 ice margins, due to sparse geochronological constraints on the ice margin, the minimum and maximum ice positions often differ by 300+ km in this region (NADI-1; Dalton et al., 2023). Discrepancies in RSL predictions made using the different ICE-NADI-1 reconstructions vary over the deglaciation. From 15 – 11 ka, for example, RSL predictions are an average of ~40 m lower in GIA simulations with ICE-NADI-1_min versus ICE-NADI-1 (Figs. 6-7, S4-S9). In contrast, average RSL predictions are ~40 m higher in simulations adopting ICE-NADI-1_max versus ICE-NADI-1 from 15 – 11 ka. Differences among the average RSL predictions made using the ICE-NADI-1 reconstructions increase from 15-11 ka because it is a time period of Laurentide ice margin retreat, and correspondingly ice sheet thinning, progresses quite differently among the three ICE-NADI-1 reconstructions (Fig. 3). Laurentide retreat and thinning progresses much more rapidly in ICE-NADI-1_min compared to ICE-NADI-1 and ICE-NADI-1_max, leading to an earlier drop in RSL as the solid Earth responds sooner to the retreating ice sheet.

The eastern Canadian coastline was almost entirely covered by the Laurentide Ice Sheet prior to the deglaciation (Fig. 2), and we find that discrepancies in RSL predictions among GIA simulations using the three ICE-NADI-1 reconstructions decrease with distance from formerly glaciated regions. Along the Atlantic Coast of the United States, in regions with RSL observations (Engelhart & Horton, 2012), differences in average RSL predictions from 16 ka to present-day reach up to ~7 m between simulations using ICE-NADI-1_min and ICE-NADI-1 and ~9 m between simulations using ICE-NADI-1_max and ICE-NADI-1 (Figs. 6, S10-S12). Like the eastern Canadian coastline, differences in RSL predictions among simulations with the ICE-NADI-1 reconstructions increase from 15-11 ka, coinciding with a period of rapid Laurentide Ice Sheet retreat, with average RSL predictions differences of ~13 m between ICE-NADI-1 and both ICE-NADI-1_min and ICE-NADI-1_max. In regions with RSL observations on the Pacific Coast of central North America (Engelhart et al., 2015), differences in average RSL predictions from 16 ka to present-day reach up to only ~2 m between GIA simulations adopting ICE-NADI-1 versus ICE-NADI-1_min or ICE-NADI-1_max (Fig. S13-S14).

From 15-11 ka, across regions 1-7 in the Hudon Bay, we find ~10 m average difference in RSL predictions among the three ICE-NADI-1 reconstructions (Fig. S4-S5). Along the northern Atlantic coast – specifically in regions 12-33 of the Vacchi et al. (2018) compilation and all regions of the Engelhart & Horton (2012) compilation – we find an average RSL prediction difference of ~37 m between the ICE-NADI-1 reconstruction and both the ICE-NADI-1_min and ICE-NADI-1_max reconstructions from 15- 11 ka, yielding an overall average RSL prediction spread of ~74 m across this time period. Differences in average RSL predictions are lower along the Pacific coast, ranging from 3 m to 8 m in regions with RSL observations (Figs. S13-S14).

Text S3. Paleotopography

In Alaska, the Cordilleran Ice Sheet margin extent and thicknesses vary substantially among the three ICE-NADI-1 reconstructions (Figs. 2-3), leading to discrepant paleotopography predictions (Fig. 9). The ICE-NADI-1_max reconstruction has a broader extent and thicker ice across southcentral Alaska from 25 ka through the deglaciation compared to both the ICE-NADI-1 and ICE-NADI-1_min reconstructions (Figs. 2-3). The thicker and more expansive ice loading in ICE-NADI-1_max manifests in more pronounced topography changes in Sukoi Bay. Topography is ~200 m, ~110 m, and ~20 m lower in Sukoi Bay from 25 ka to ~18-16.5 ka in the ICE-NADI-1_max, ICE-NADI-1, and ICE-NADI-1_min reconstructions, respectively (Fig. 9g). All GIA simulations with the ICE-NADI-1 reconstructions predict greater subsidence in Sukoi Bay than both ICE-7G and LW-6.

The central part of Michigan lies ~350-400 km north of the Laurentide Ice Sheet's maximum southern extent in the ICE-NADI-1 and ICE-NADI-1_min reconstructions but falls just beyond the ice margin in the ICE-NADI-1_min reconstructions (Fig. 2). Ice loading in GIA simulations with ICE-NADI-1 and ICE-NADI-1_max lead to ~300 m of subsidence relative to present, whereas simulations with ICE-NADI-1_min only show ~8 m of subsidence associated with ice loading (Fig. 9i). As the Laurentide retreats, we predict up to ~30-60 m of uplift relative to present in central Michigan between ~13-6 ka, associated with the migration of the peripheral bulge. Paleotopography predictions made using ICE-7G, NAICE, and LW-6 differ only slightly from predictions made with ICE-NADI-1.

Paleotopography predictions in central Pennsylvania show how ice margin extent and thickness influence peripheral bulge development and migration. Central Pennsylvania lies within the peripheral bulge at 25 ka in the ICE-NADI-1_min reconstruction, whereas the region sat just beyond the southern maximum extent of the Laurentide in the ICE-NADI-1 and NADI-1_max reconstructions (Fig. 2). Thus, the growth and subsequent collapse of the peripheral bulge, reaching up to ~70 m elevation, is evident in central Pennsylvania in GIA simulations using the ICE-NADI-1 and ICE-NADI-1_max reconstructions (Fig. 9j).

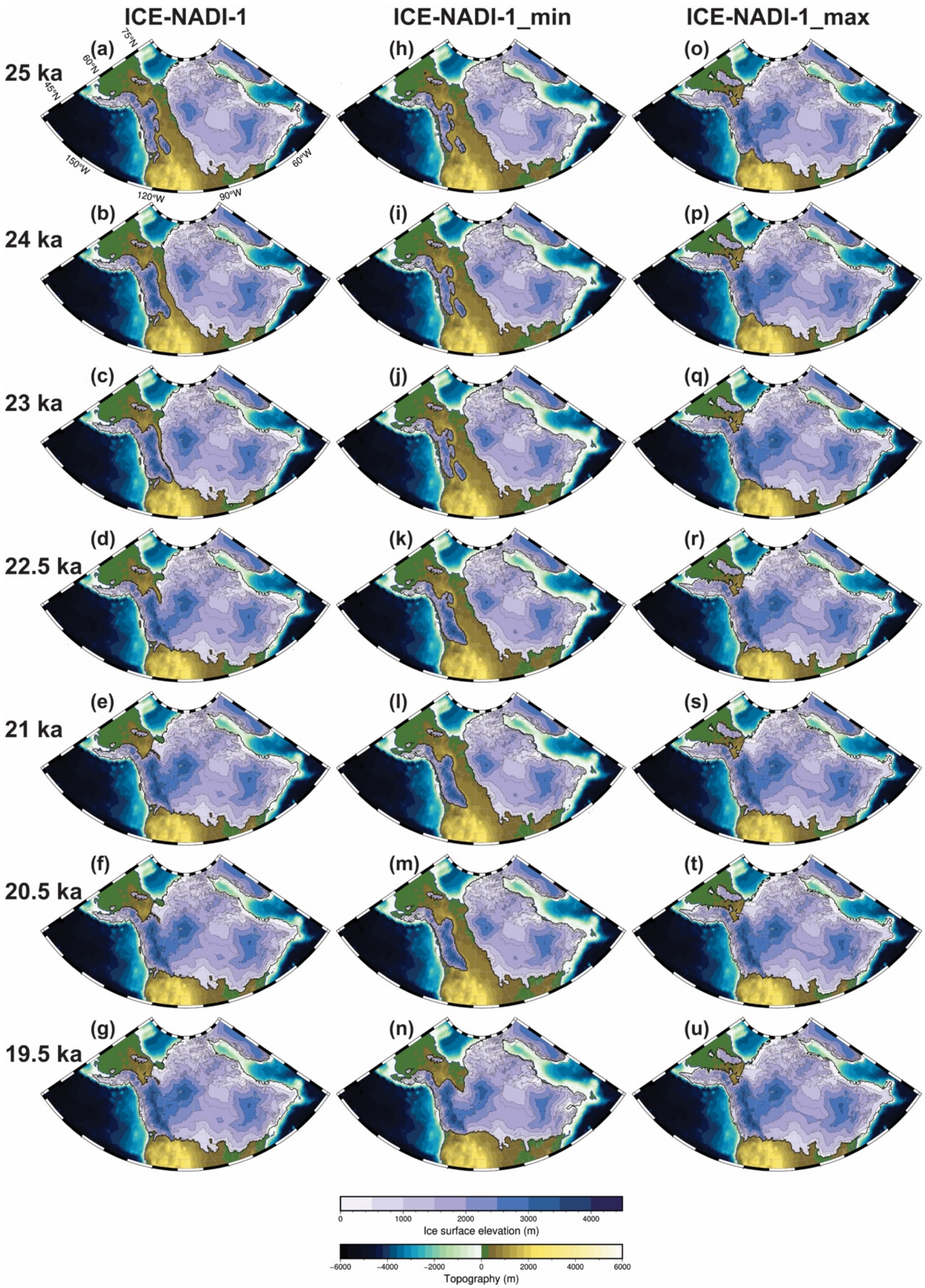

Figure S1. Ice surface elevation at 25, 24, 23, 22.5, 21, 20.5, and 19.5 ka in the (a-g) ICE-NADI-1, (h-n) ICE-NADI-1_min, and (o-u) ICE-NADI-1_max reconstructions using the Earth_1 model. Paleotopography is shown beneath the ice surface elevation for each time step. Coastlines corresponding to each time step are outlined in dark blue, while modern coastlines and state/provincial boundaries are included for reference.

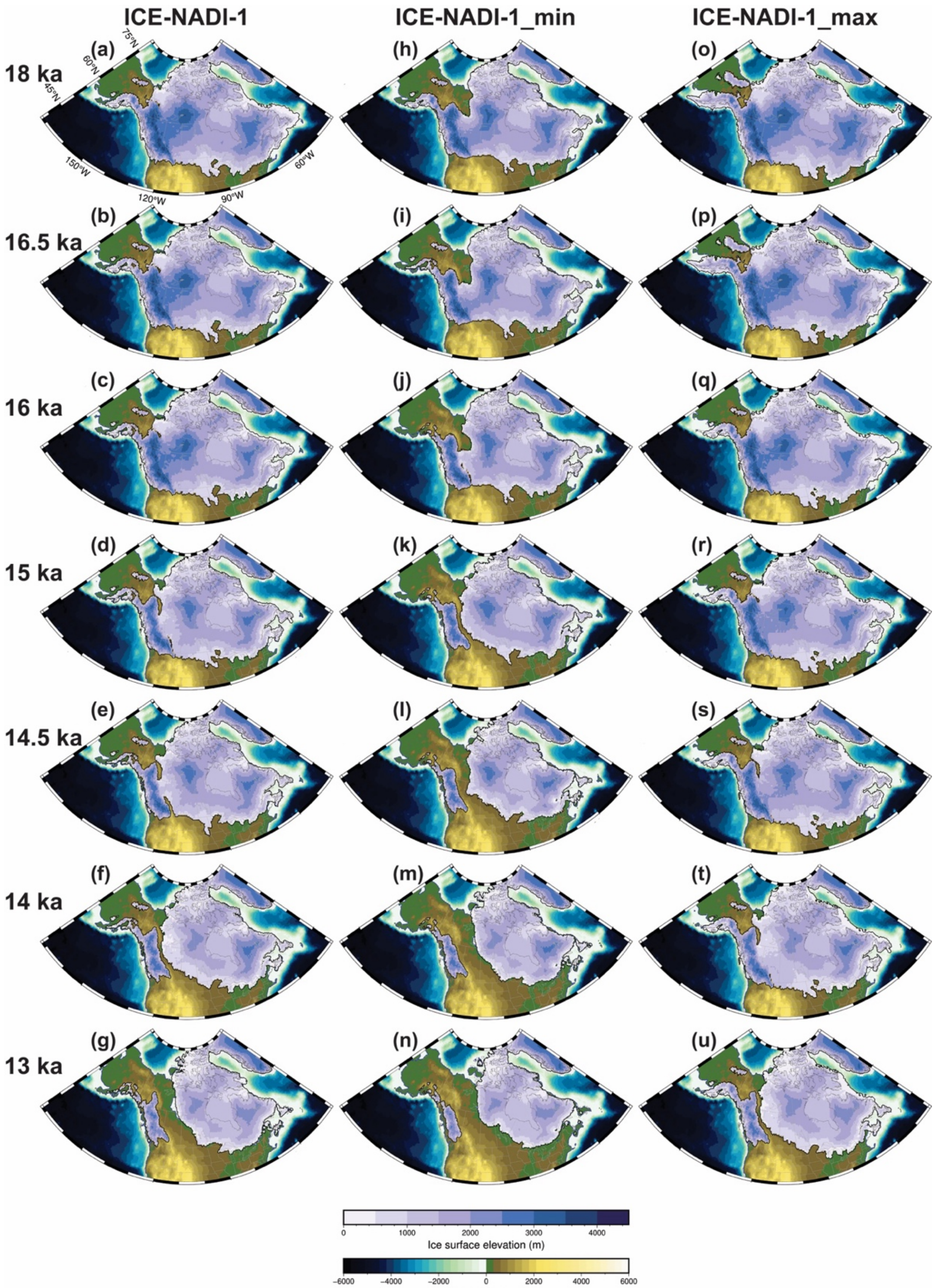

Figure S2. Ice surface elevation at 18, 16.5, 16, 15, 14.5, 14, and 13 ka in the (a-g) ICE-NADI-1, (h-n) ICE-NADI-1_min, and (o-u) ICE-NADI-1_max reconstructions using the Earth_1 model. Paleotopography is shown beneath the ice surface elevation for each time step. Coastlines corresponding to each time step are outlined in dark blue, while modern coastlines and state/provincial boundaries are included for reference.

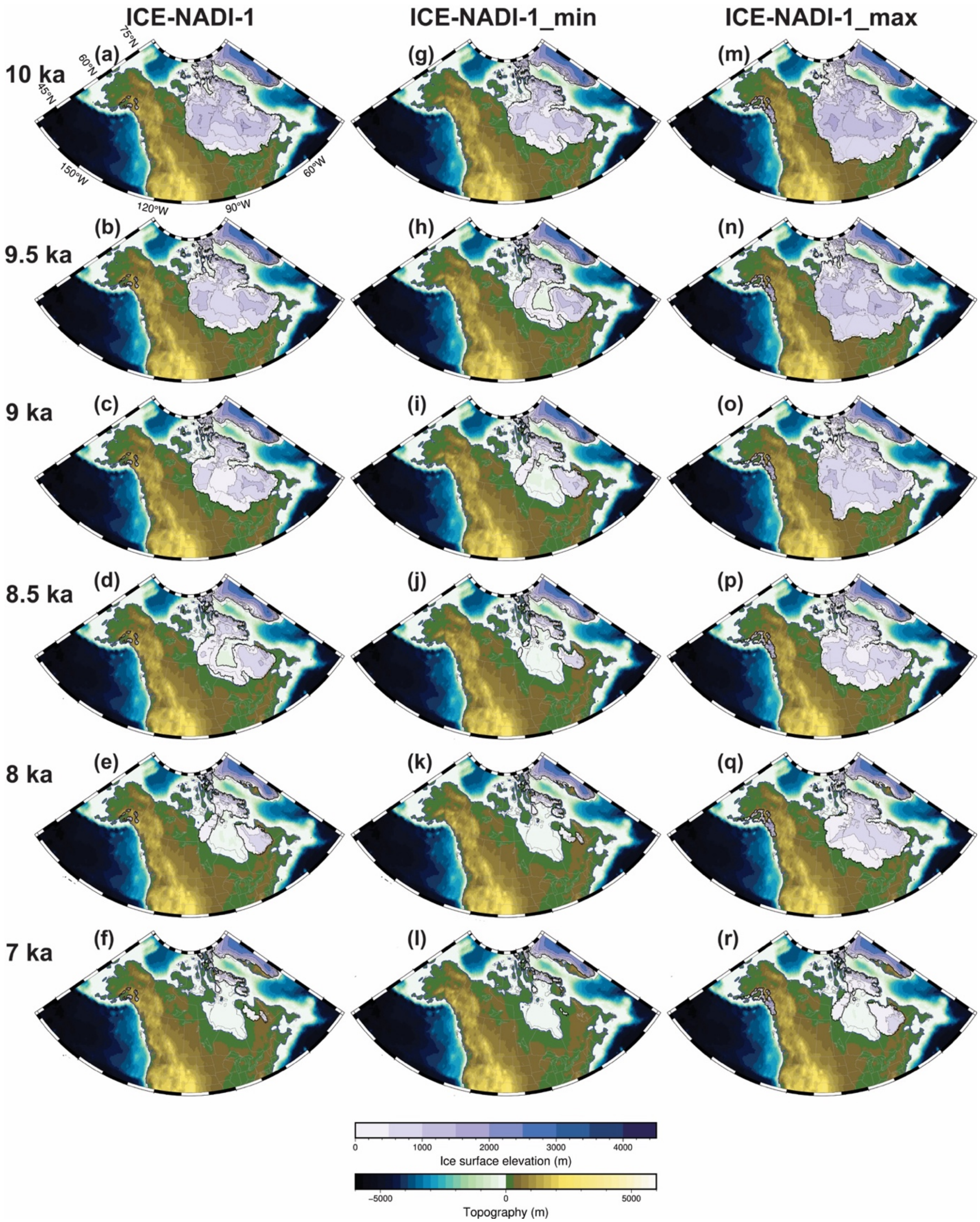

Figure S3. Ice surface elevation at 10, 9.5, 9, 8.5, 8, 7 ka in the (a-b) ICE-NADI-1, (d-f) ICE-NADI-1_min, and (g-i) ICE-NADI-1_max reconstructions using the Earth_1 model. Paleotopography is shown beneath the ice surface elevation for each time step. Coastlines corresponding to each time step are outlined in dark blue, while modern coastlines and state/provincial boundaries are included for reference.

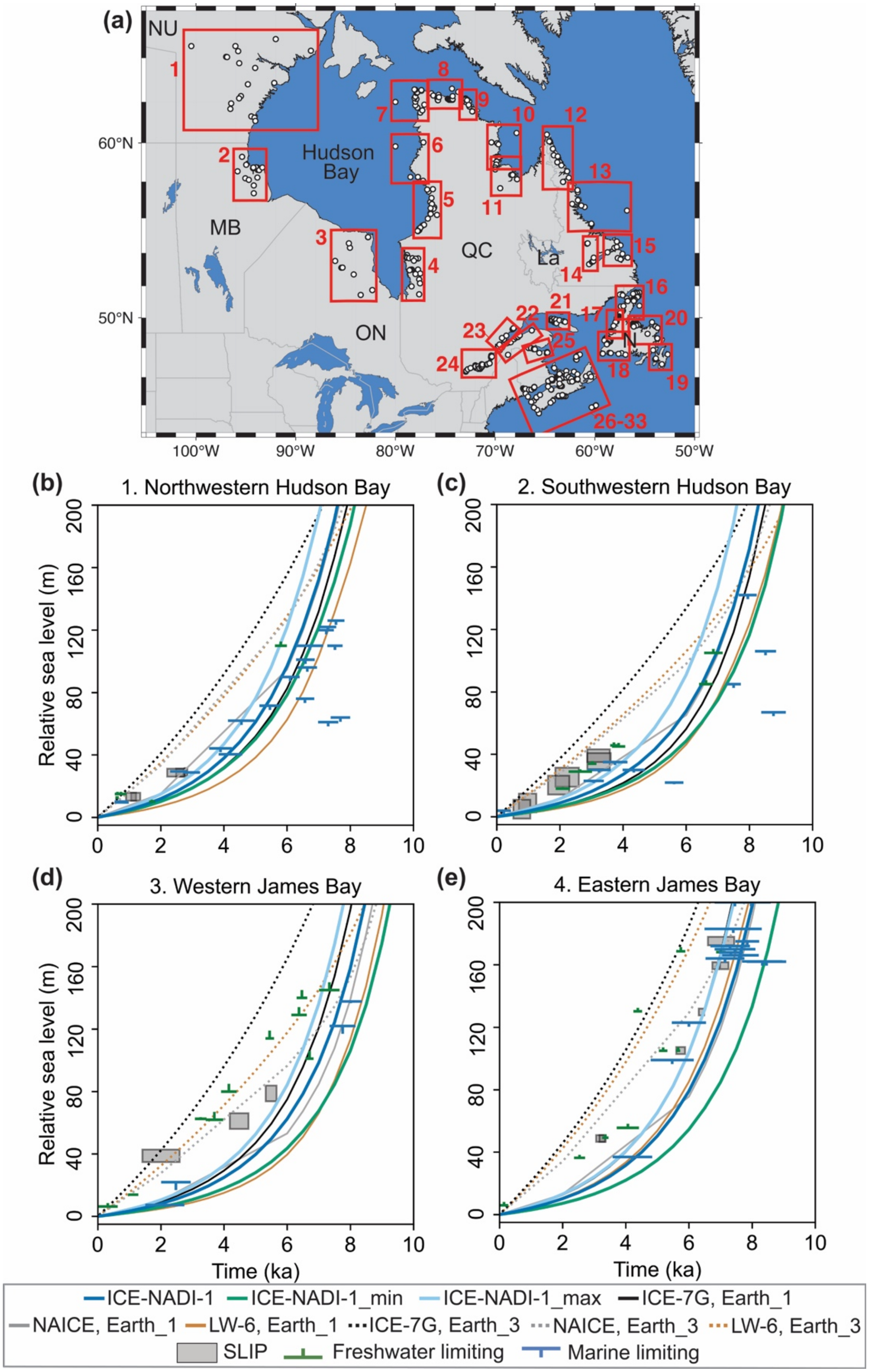

(a)
NU
MB
Hudson Bay
QC
La
ON
N
60°N
50°N
100°W
90°W
80°W
70°W
60°W
50°W
1
2
3
4
5
6
7
8
9
10
11
12
13
14
15
16
17
18
19
20
21
22
23
24
25
26-33
(b)
1. Northwestern Hudson Bay
(c)
2. Southwestern Hudson Bay
(d)
3. Western James Bay
(e)
4. Eastern James Bay
Relative sea level (m)
Time (ka)
ICE-NADI-1
ICE-NADI-1_min
ICE-NADI-1_max
ICE-7G, Earth_1
NAICE, Earth_1
LW-6, Earth_1
ICE-7G, Earth_3
NAICE, Earth_3
LW-6, Earth_3
SLIP
Freshwater limiting
Marine limiting

Figure S4. RSL data-model comparison along the eastern Canadian coastline. (a) Map showing the spatial distribution of RSL data from the Vacchi et al. (2018) compilation. The data are grouped into 34 regions, select regions are also shown in the main text in Figs. 6-7. White circles mark the location of individual RSL observations. Abbreviations: NU: Nunavut, MB: Manitoba, ON: Ontario, QC: Quebec, La: Labrador, N: Newfoundland. (b-e) Data-model comparison for regions 1, 2, 3, and 4 shown in (a). Data-model comparisons for the other regions shown in (a) are plotted in Figs. S5-S9. The Earth_1 model is used for sea level predictions with all the ICE-NADI-1, ICE-NADI-1_max, ICE-NADI-1_min reconstructions as well as the ICE-7G, LW-6, and NAICE reconstructions (solid lines). We also plot RSL predictions made using ICE-7G, LW-6, and NAICE with the Earth_3 model (dashed lines). We specifically adopt the Earth_3 model because it is identical to the viscoelastic Earth model used by Gowan et al. (2016b) for the NAICE reconstruction and is comparable to the VM7 model associated with ICE-7G, which has average upper and lower mantle viscosities of 4.5×10^{20} Pa s and 7.45×10^{22} Pa s, respectively (Roy & Peltier, 2017).

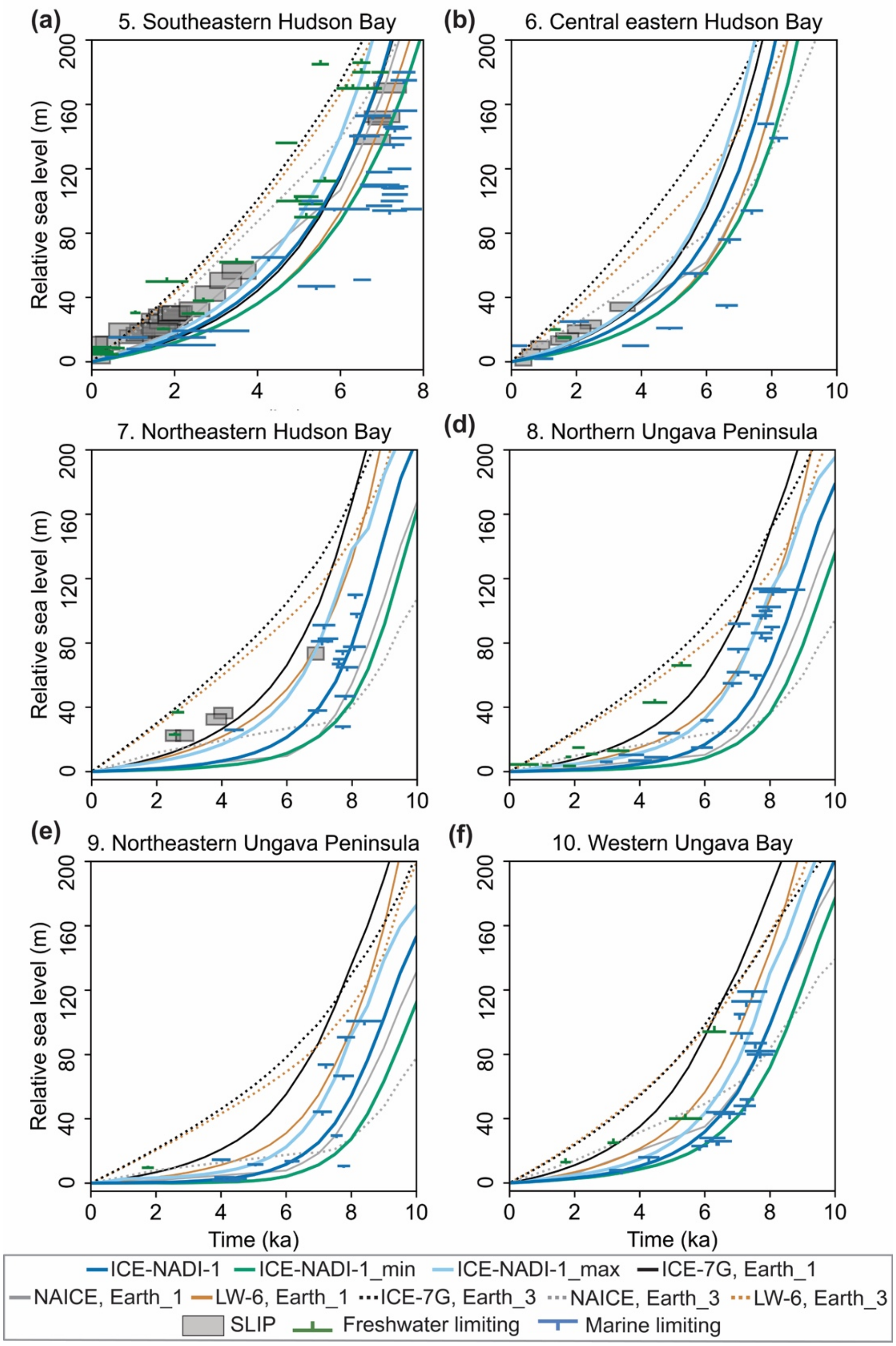

Figure S5. RSL data-model comparison for regions 5-10 from Fig. S4a on the eastern Canadian coastline. See the caption of Fig. S4 for additional details.

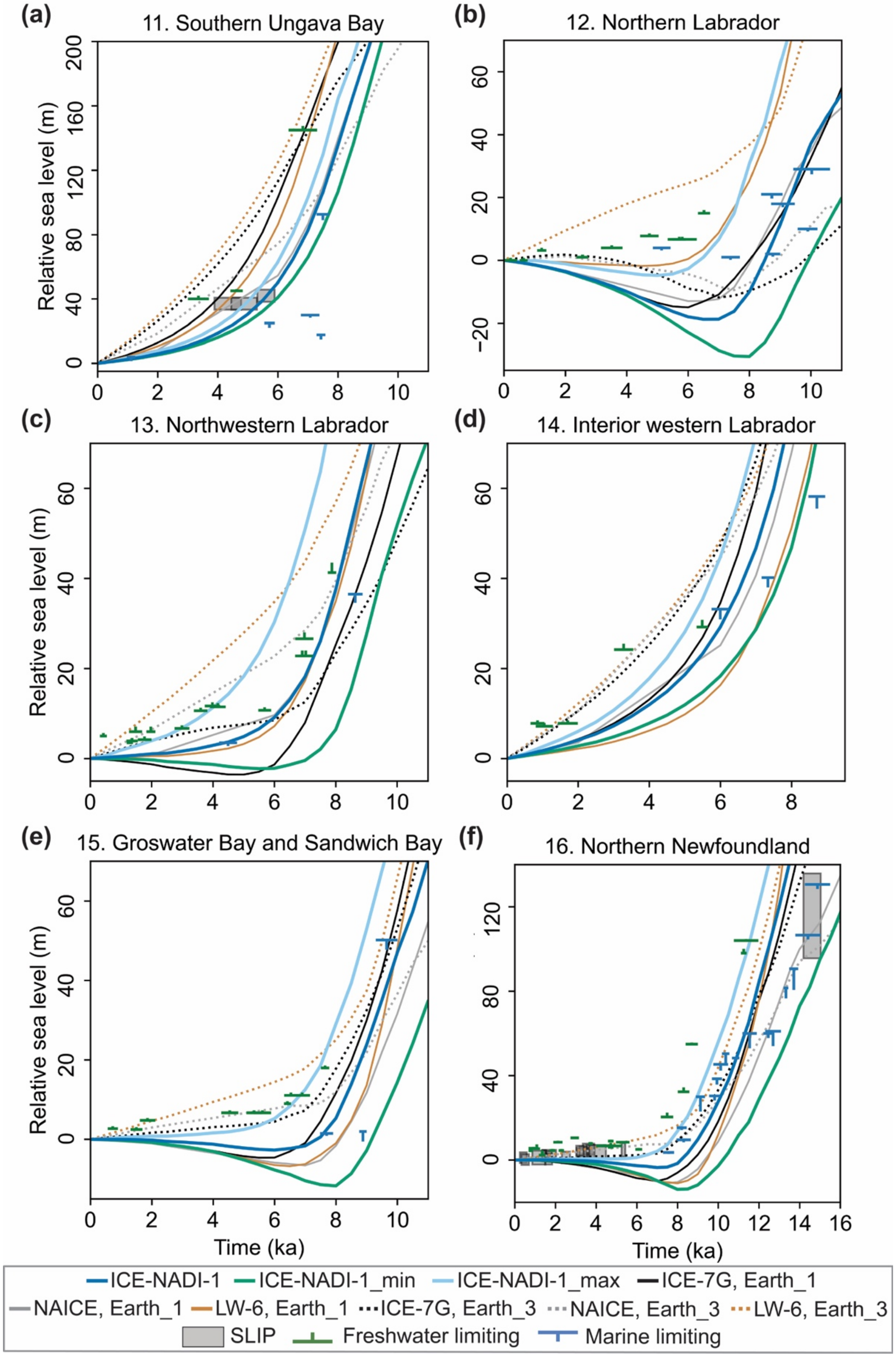

Figure S6. RSL data-model comparison for regions 11-16 from Fig. S4a on the eastern Canadian coastline. See the caption of Fig. S4 for additional details.

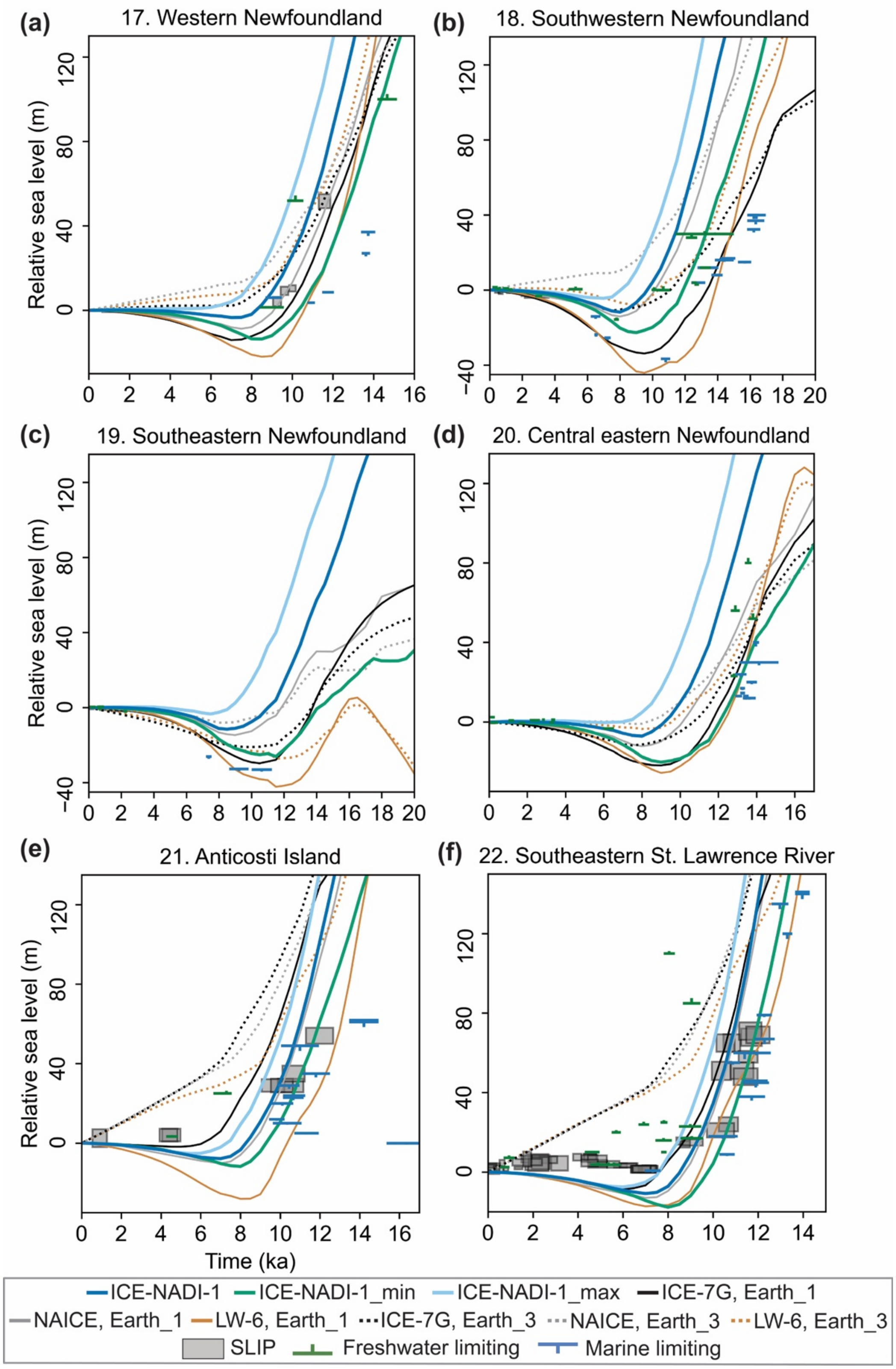

Figure S7. RSL data-model comparison for regions 17-22 from Fig. S4a on the eastern Canadian coastline. See the caption of Fig. S4 for additional details.

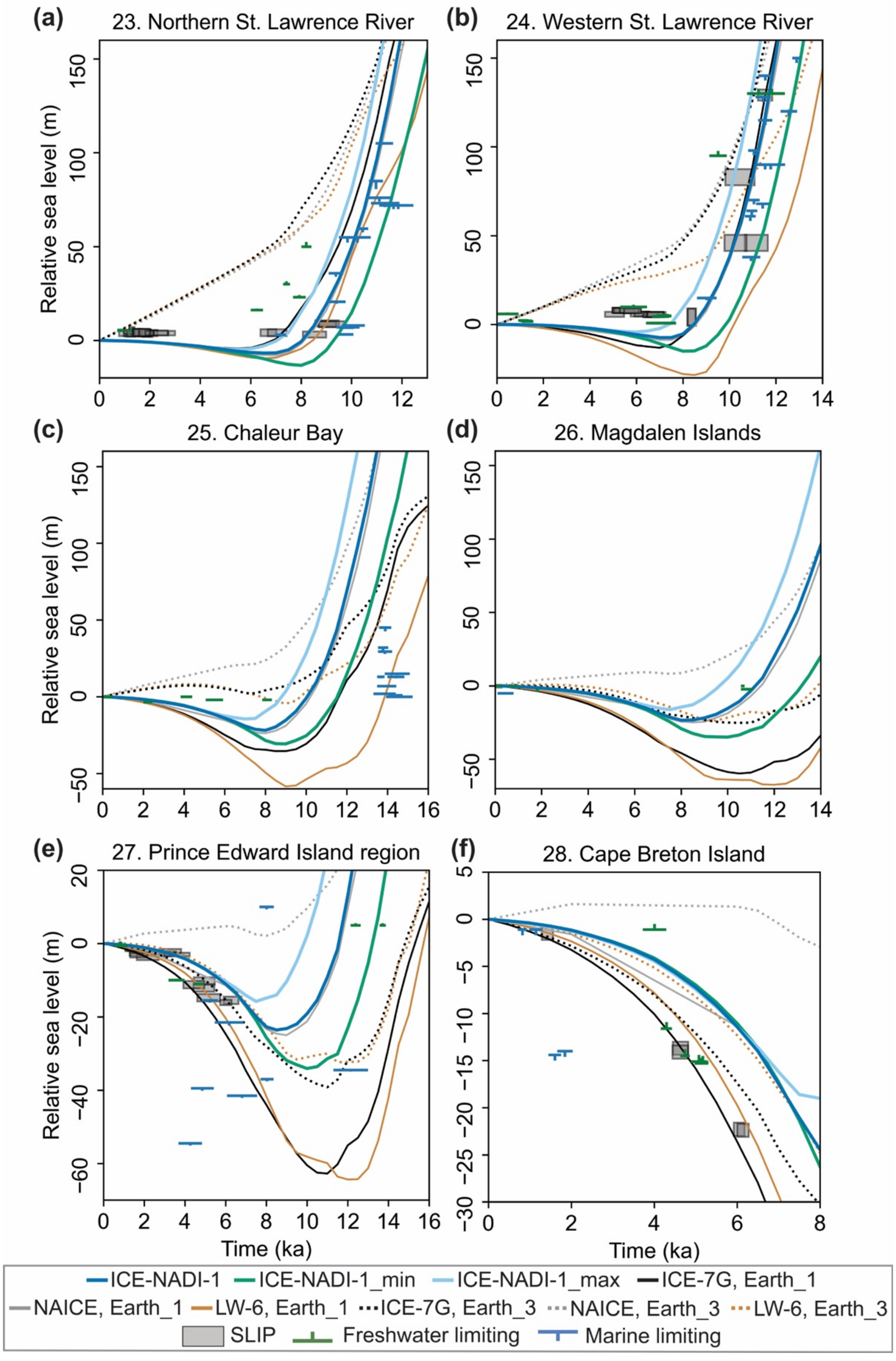

Figure S8. RSL data-model comparison for regions 23-28 from Fig. S4a on the eastern Canadian coastline. See the caption of Fig. S4 for additional details.

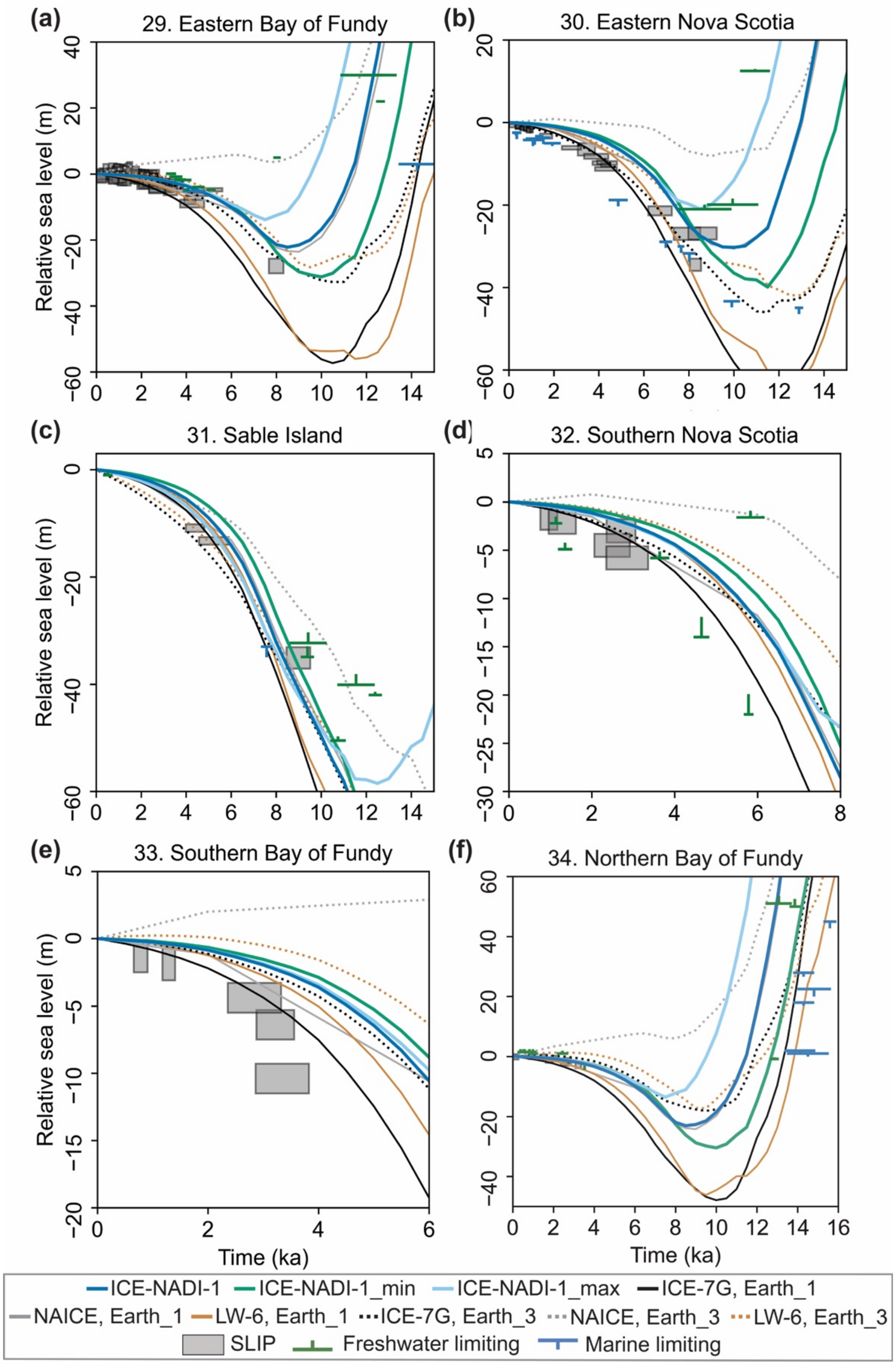

Figure S9. RSL data-model comparison for regions 29-34 from Fig. S4a on the eastern Canadian coastline. See the caption of Fig. S4 for additional details.

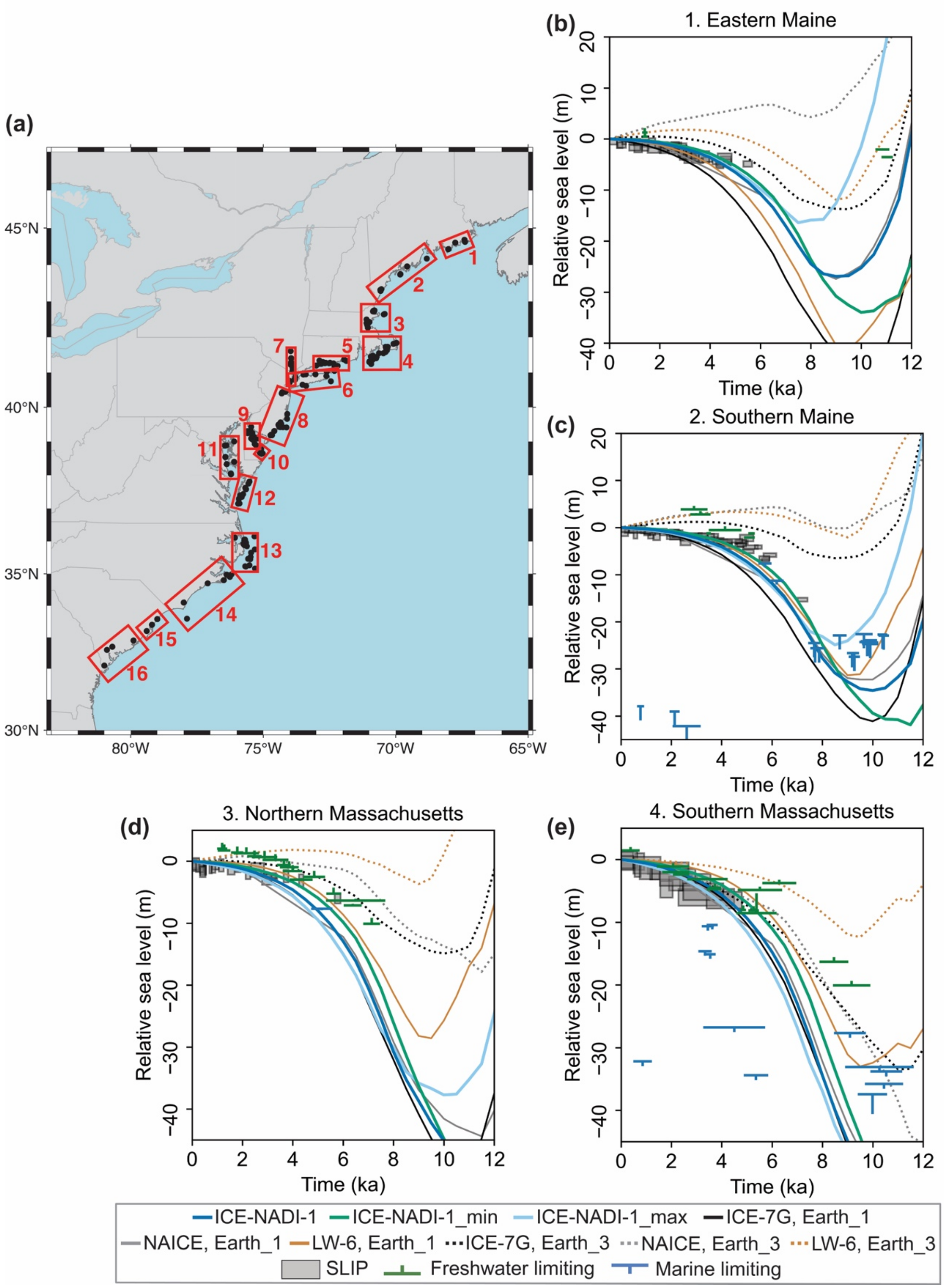

Figure S10. RSL data-model comparison along Atlantic Coast of the United States. (a) Map showing the spatial distribution of RSL data from the Engelhart & Horton (2012) compilation. The data are grouped into 16 regions, select regions are also shown in the main text in Figs. 6-7.

Black circles mark the location of individual RSL observations. Data-model comparison for regions 1, 2, 3, and 4 shown in (a). Data-model comparisons for the other regions shown in (a) are plotted in Figs. S11-S12. The Earth_1 model is used for sea level predictions with the ICE-NADI-1, ICE-NADI-1_max, and ICE-NADI-1_min reconstructions as well as the ICE-7G, LW-6, and NAICE reconstructions (solid lines). We also plot RSL predictions made using ICE-7G, LW-6, and NAICE with the Earth_3 model (dashed lines). We specifically adopt the Earth_3 model because it is identical to the viscoelastic Earth model used by Gowan et al. (2016b) for the NAICE reconstruction and is comparable to the VM7 model associated with ICE-7G, which has average upper and lower mantle viscosities of 4.5×10^{20} Pa s and 7.45×10^{22} Pa s, respectively (Roy & Peltier, 2017).

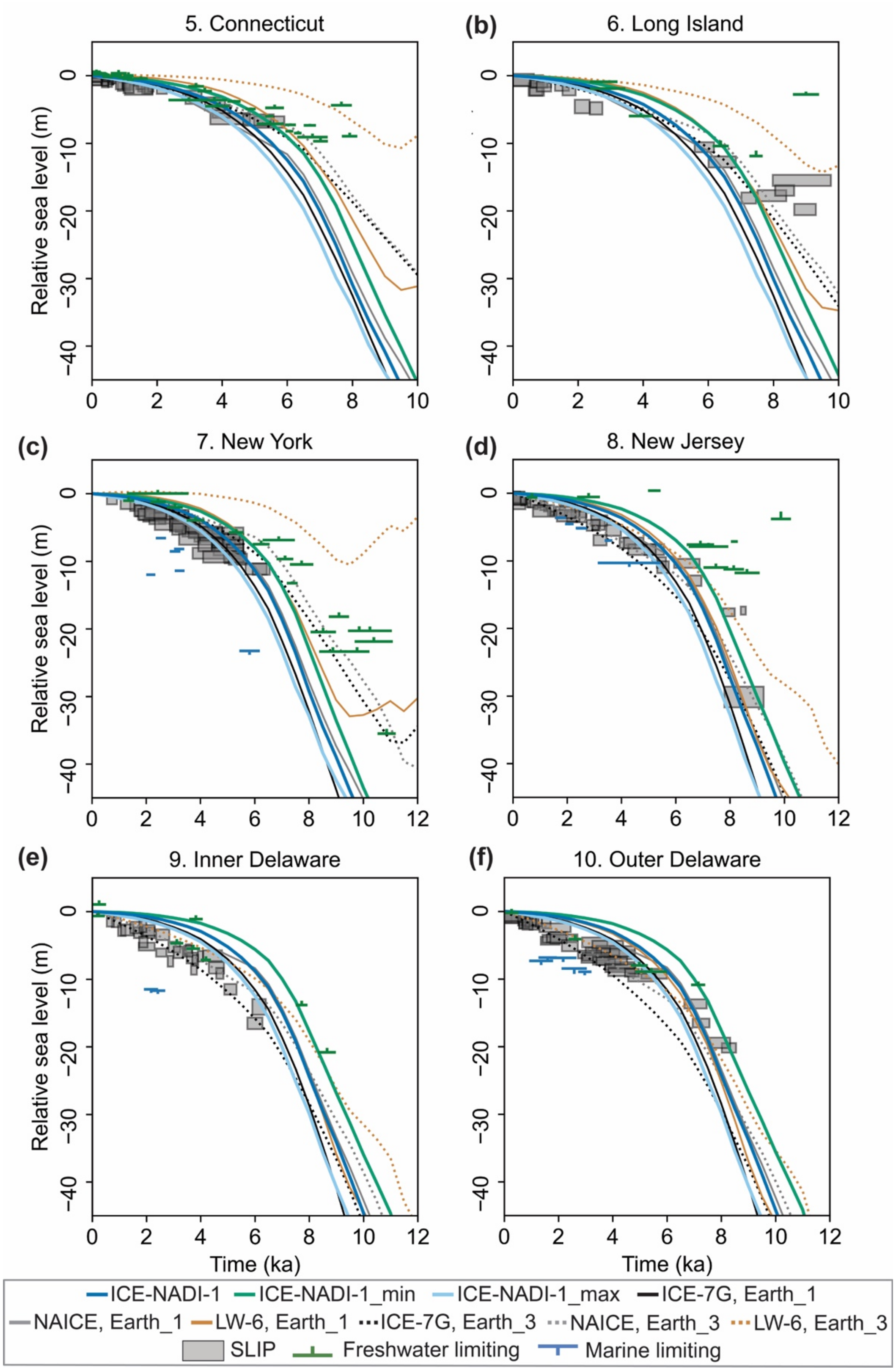

Figure S11. RSL data-model comparison for regions 5-10 from Fig. S10a on the Atlantic Coast of the United States. See the caption of Fig. S10 for additional details.

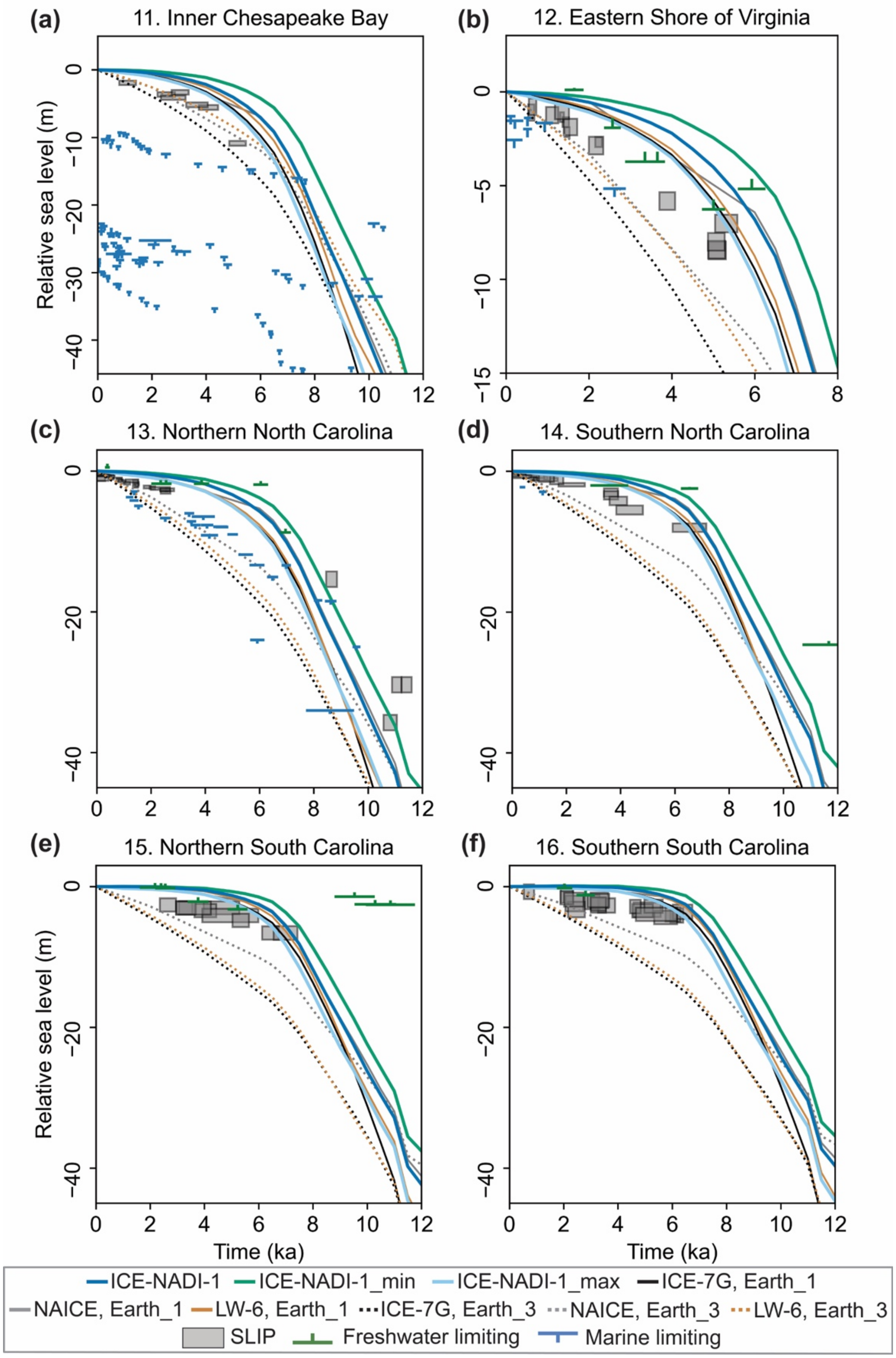

Figure S12. RSL data-model comparison for regions 11-16 from Fig. S10a on the Atlantic Coast of the United States. See the caption of Fig. S10 for additional details.

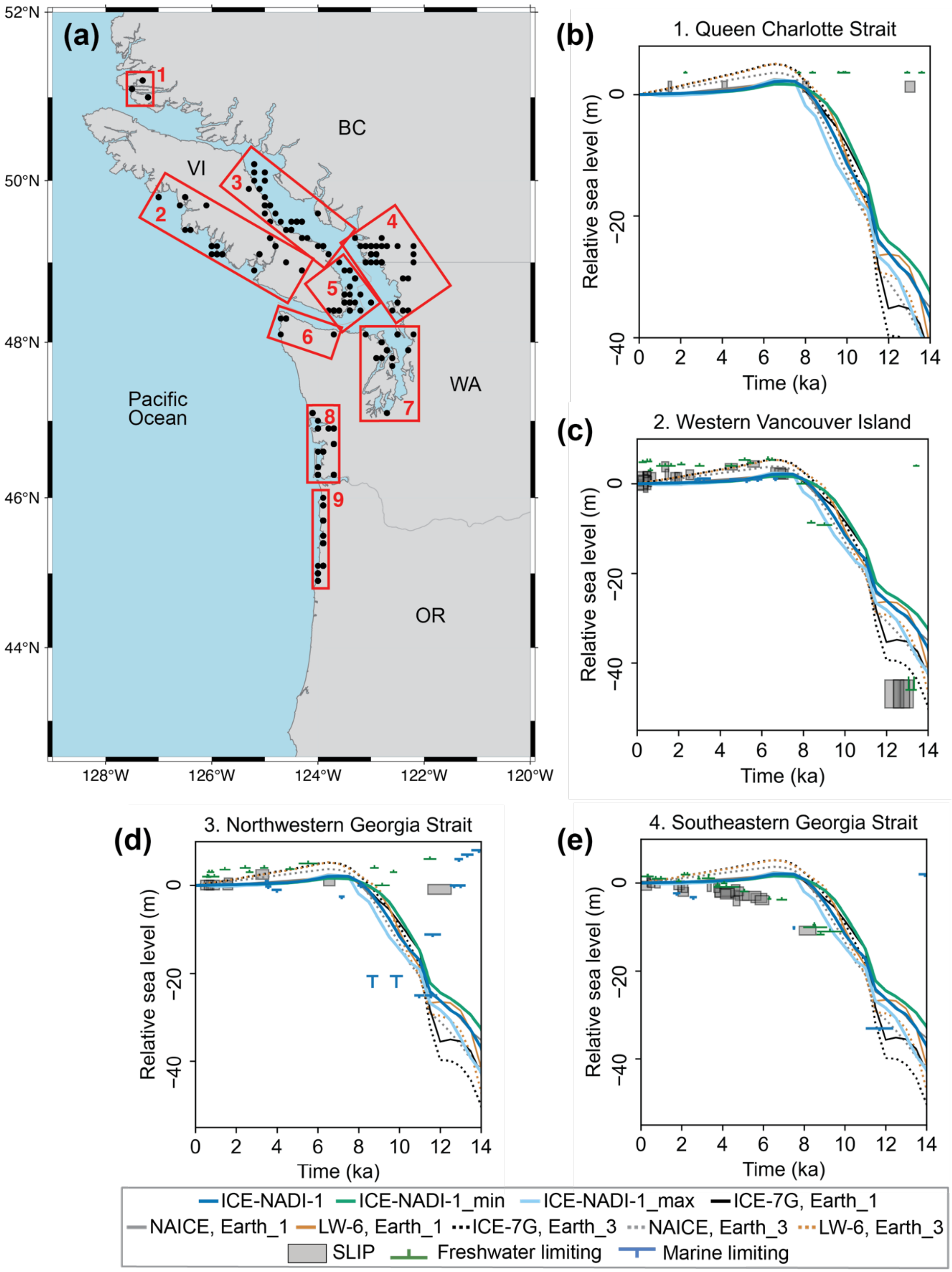

Figure S13. RSL data-model comparison along the Pacific Coast of central North America. (a) Map showing the spatial distribution of RSL data from regions 1-9 of the Engelhart et al. (2015) compilation for British Columbia (BC), Washington (WA), and Oregon (OR). Black circles mark the location of individual RSL observations. Vancouver Island (VI) is labeled. As in

Yousefi et al. (2018), a tectonic correction is not applied to RSL data in regions 1-9 of the Engelhart et al. (2015) compilation. (b-e) Data-model comparison for regions 1, 2, 3, and 4 shown in (a). Data-model comparisons for the other regions shown in (a) are plotted in Fig. S14. The Earth_1 model is used for sea level predictions with all the ICE-NADI-1, ICE-NADI-1_min, and ICE-NADI-1_max reconstructions as well as the ICE-7G, LW-6, and NAICE reconstructions (solid lines). We also plot RSL predictions made using ICE-7G, LW-6, and NAICE with the Earth_3 model (dashed lines).

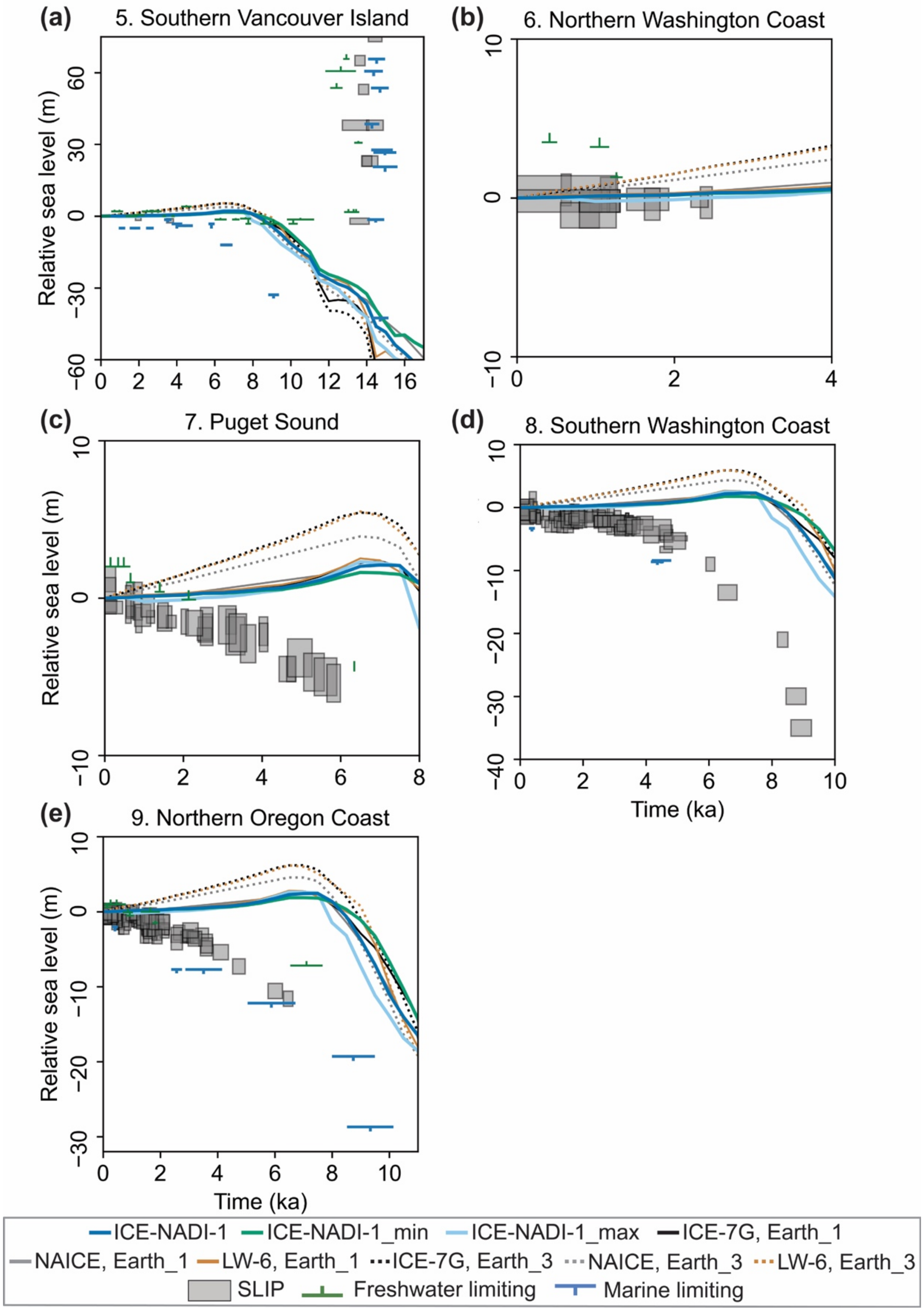

Figure S14. Data-model comparison for regions 5-9 from Fig. S13a along the Pacific Coast of central North America. See the caption of Fig. S13 for additional details.